

See discussions, stats, and author profiles for this publication at:  
<https://www.researchgate.net/publication/231362672>

# Synchrotron radiation photoemission study of some $\pi$ -conjugated alkynes in the gas phase: Experiment and theory

ARTICLE *in* CHEMICAL PHYSICS · FEBRUARY 2001

Impact Factor: 1.65 · DOI: 10.1016/S0301-0104(00)00396-7

CITATIONS

17

READS

18

7 AUTHORS, INCLUDING:



**Vincenzo Carravetta**

Italian National Research Council

207 PUBLICATIONS 3,271 CITATIONS

SEE PROFILE



**Maria Vittoria Russo**

Sapienza University of Rome

210 PUBLICATIONS 2,963 CITATIONS

SEE PROFILE



**Stefano Stranges**

Sapienza University of Rome

136 PUBLICATIONS 1,416 CITATIONS

SEE PROFILE



**Monica De Simone**

Italian National Research Council

108 PUBLICATIONS 931 CITATIONS

SEE PROFILE

# Synchrotron radiation photoemission study of some $\pi$ -conjugated alkynes in the gas phase: Experiment and theory

V. Carravetta <sup>a,\*</sup>, G. Iucci <sup>b</sup>, A. Ferri <sup>c</sup>, M.V. Russo <sup>c</sup>, S. Stranges <sup>c,d</sup>,  
M. de Simone <sup>b</sup>, G. Polzonetti <sup>b</sup>

<sup>a</sup> ICQEM, Area della Ricerca del CNR, via Alfieri 1, I-56010 San Giuliano Terme (PI), Italy

<sup>b</sup> Dipartimento di Fisica, Università di Roma Tre e Unita' INFM di Roma Tre, Via della Vasca Navale 79, 00146 Rome, Italy

<sup>c</sup> Dipartimento di Chimica, Università di Roma "La Sapienza", P.le A. Moro 5, 00185 Rome, Italy

<sup>d</sup> Unità INFM, Università di Roma "La Sapienza", P.le A. Moro 5, 00185 Rome, Italy

Received 24 July 2000; in final form 13 October 2000

## Abstract

C1s core level photoelectron studies have been performed in the gas phase for some conjugated organic molecules, namely phenylacetylene, diethynylbiphenyl, diphenylbutadiyne and *para*-nitrophenylacetylene. The investigated systems consist of alkyne molecules with aromatic substituents and have been used as precursors for the synthesis of organic  $\pi$ -conjugated polymers. The experimental results were interpreted with the help of theoretical calculations: the ionization potentials have been predicted for all the chemically different carbon atoms of the organic molecules by means of  $\Delta$ SCF quantum chemical calculations and compared with the measured binding energies of the various features present in the experimental spectra. A good agreement between experiment and theory was found. © 2001 Elsevier Science B.V. All rights reserved.

## 1. Introduction

During the last decades, the use of organic  $\pi$ -conjugated polymers in electronic devices has stimulated the research on the preparation and characterization of these interesting materials [1]. Poly-monosubstituted acetylenes (general formula  $[-CH=CR-]_n$ , R = pendant group), for instance, have been studied as sensing membranes in gas-sensor devices both of resistive [2,3] and of sensor acoustic wave (SAW) type [4] and for third order non linear optical properties [5]. Various

$\pi$ -conjugated polymers containing aromatic substituents as pendant groups (e.g. polyphenylacetylene R = C<sub>6</sub>H<sub>5</sub>; poly(*para*-nitrophenylacetylene) R = *p*-C<sub>6</sub>H<sub>4</sub>NO<sub>2</sub>) have been synthesized from the corresponding alkynes (R–C $\equiv$ CH with: R = C<sub>6</sub>H<sub>5</sub>, phenylacetylene (PA); R = *p*-C<sub>6</sub>H<sub>4</sub>NO<sub>2</sub>, *para*-nitrophenylacetylene) via opening of the triple bond and subsequent formation of a conjugated polymer backbone [6,7]; the reaction is catalyzed by transition metal complexes.

In connection with the use of polyphenylacetylene as gas-sensing membrane in electronic devices, the polymer surface has been extensively studied by surface sensitive techniques such as X-ray photoemission spectroscopy (XPS) [8] and near-edge X-ray absorption fine structure spectroscopy

\* Corresponding author.

E-mail address: carra@indigo.icqem.pi.cnr.it (V. Carravetta).

(NEXAFS) [9]; the interaction of the polymer surface with gas molecules [8] and the interface formation with deposited metals such as copper [10,11] and chromium [12] were also investigated by XPS.

Poly-yne polymers containing transition metals in the main chain are another class of  $\pi$ -conjugated materials of great interest for molecular electronics, due to their peculiar physical properties, such as third-order non linearity and photoluminescence [13,14]. For instance, Pt- and Pd-organo-metallic polymers containing the metals inserted in the main chain by  $\sigma$ -bonding between diethynylbiphenyl (DEBP) units have been used in the preparation of gas sensing devices [15]. The study of the molecular structure of these complex polymeric materials by means of XPS [16] and NEXAFS [17] techniques was recently reported by some of us. The NEXAFS spectra evidenced an unexpected alignment of the polymer chains even in thick (some microns) films. The interpretation of the polymer spectra is, of course, very complicated.

In order to gain an insight into the chemical and electronic structure of polymeric materials, we think that the study of simple organic molecules, that can be used as models for the more complex polymeric structures, can supply useful information. Small organic molecules, whose XPS spectra are better resolved and easier to interpret, have been extensively used for the interpretation of the photoemission spectra of polymers, as it has been recently reviewed by Beamson and Briggs [18]. Comparison with the XPS spectra of methane, for instance shed light on the vibrational structure of solid state long-chain hydrocarbons [18]. Naves de Brito et al. reported joint experimental and theoretical studies of the XPS spectra of gas phase organic acids and esters used as models for polymethylmethacrylate [19], and of simple nitriles studied as models for the interpretation of the XPS spectrum of polyacrylonitrile [20].

In a previous paper [21], some of us reported the NEXAFS C K-edge spectrum of gas phase PA; the experimental data have been interpreted with the help of quantum chemical calculations, predicting the ionization potentials and the theoretical C K-edge NEXAFS spectrum for the six

non-equivalent carbon atoms of this molecule. In the framework of the above described approach, we present here a joint experimental and theoretical investigation on the electronic structure of some  $\pi$ -conjugated alkyne molecules, whose chemical structure is shown in Fig. 1: PA, 4,4'-diethynylbiphenyl (DEBP), diphenylbutadiyne (DPBD) and *para*-nitrophenylacetylene (PNPA). For all the investigated molecules six non-equivalent sets of carbon atoms can be found, labeled 1–6 in the figure. DEBP and DPBD can be considered as derived by two PA molecules linked together through the benzene ring in the *para* position (C6) and through the triple bonds (C1), respectively. Moreover, DEBP has been used in the preparation

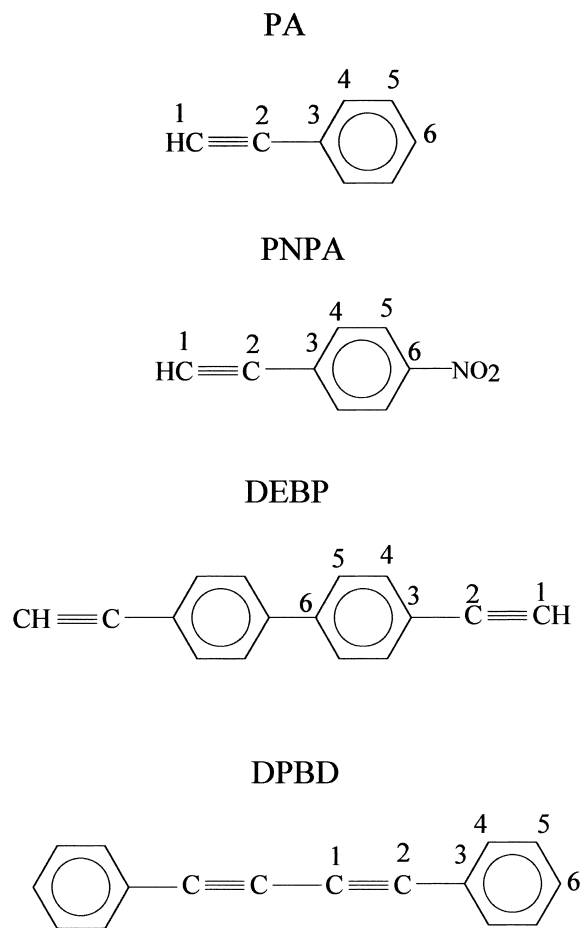


Fig. 1. Chemical structure of the investigated molecules; the non-equivalent carbon atoms are labeled 1–6 in the figure.

of the Pt- and Pd-organometallic polymers containing the DEBP moiety  $\sigma$ -bonded through the alkyne group to platinum and palladium [22].

The gas phase C1s photoemission spectra have been recorded and compared with the ionization potentials determined for the six non-equivalent carbon atoms of the investigated molecules by  $\Delta$ SCF quantum chemical calculations. The information obtained from the gas phase spectra of these simple organic molecules will be used in the interpretation of the NEXAFS spectra first of the same model molecules and successively of the more complex polymeric systems.

## 2. Experimental

Diethynylbiphenyl (DEBP) [23], diphenylbutadiyne (DPBD) [24] and *para*-nitrophenylacetylene [25] were prepared according to published methods; PA (commercial product, Fluka) was distilled prior to use.

C1s X-ray photoelectron spectra were recorded at the ARPES end-station of the Gas Phase Photoemission Beamline of Elettra [26]. The volatile liquid sample (PA) was introduced into the ionization region through a hypodermic needle mounted on a XYZ manipulator. The solid samples (PNPA, DEBP, DPBD) were vaporized from a stainless steel crucible whose temperature was read by a thermocouple and kept constant within 1–2 degrees during the measurements. Vaporization temperatures for the solid samples ranged from 35°C to 90°C. The resistively heated oven and the ionization volume were enclosed in a liquid nitrogen cooled jacket.

The VSW hemispherical photoelectron energy analyzer employed (50 mm mean radius) was enclosed in a double  $\mu$ -metal shield and operated with 5 and 25 eV pass energies for the liquid and the three solid samples, respectively. The total instrumental resolution (monochromator plus electron analyzer) was about 0.3 eV for the liquid and 0.4 eV for the solid samples. The 4-element lens system of the analyzer was modified to suit high temperature experiments and the active surfaces were heated to minimize coating and charging effects. All spectra were recorded at 337.0 eV photon

energy. The energy-analyzed electrons were detected by a single channeltron multiplier. All experimental spectra were calibrated using the Ar2p<sub>3/2</sub> line at 248.4 eV ionization energy.

Curve-fitting deconvolution of the experimental spectra was performed by using gaussian curves as fitting functions. The BEs of the component peaks were chosen on the basis of the calculated BEs for the non-equivalent sets of carbon atoms (see Section 3). The area ratios between the fitting components were kept fixed and equal to the atomic ratios between the corresponding non-equivalent carbon atoms (the C1s photoelectron cross-section being constant). The FWHM was reasonably assumed to be the same for all the fitting components (approximately  $\sim 0.4$  eV); peaks corresponding to more than one non-equivalent set of carbon atoms having BEs very close to each other were assumed to be 0.1–0.2 eV larger. Further details are explained in Section 4. The coefficient of determination ( $r^2$ ) in all the fits was higher than 0.99.

## 3. Computational

The analysis of a molecular XPS spectrum is usually performed by a theoretical model in which validity of the MO model, electron relaxation, electron correlation, vibrational broadening, and relativistic corrections may play a role of different importance, depending, mostly, on the electron shell involved in the ionization process. In the case of core electron ionization the MO-model is substantially valid and the main correction to the band position obtained by the simple Koopman theorem approximation, is given by the electron relaxation. In the case of ionization at the C K-edge the relaxation energy amounts typically to about  $-15$  eV and it is one order of magnitude larger than the other energy corrections. For molecules, like the ones here investigated, containing non-equivalent carbon atoms to which correspond core electron binding energies (BEs) that are shifted by different chemical environments, the minor correlation effects can be considered almost the same for core ionization at non-equivalent sites. A theoretical model neglecting correlation and vibrational effects but including the electronic

relaxation around the core hole, may then be considered suitable for the analysis of the main features of a molecular core electron XPS spectrum. On this assumption we calculated the IP for each non-equivalent carbon atom by the  $\Delta$ SCF procedure, i.e. as the difference between the ground state and the core-hole state energies both obtained by direct SCF calculations using DALTON [27].

The geometry of each molecule has been optimized for the ground state at the SCF level. The equilibrium geometry for the DEBP molecule, consisting of two PA units linked together through the benzene carbons C6, a torsion angle  $\theta = 42^\circ$  between the two benzene rings, very close to the value found for biphenyl, was calculated. For  $\theta = 0^\circ$  the two phenyl rings are perfectly coplanar, allowing a complete conjugation between the two aromatic  $\pi$ -systems. However, a coplanar geometry would result in a non-bonded steric repulsion between the hydrogen atoms in the *ortho* position with respect to the  $\sigma$ -bond between the two benzene rings, i.e. bonded to C5, on the two aromatic rings. Apparently, the energy gain due to the removal of the steric interaction between the non-bonded hydrogens in the *ortho* position is higher than the energy gain resulting from the extended  $\pi$ -conjugation between the two aromatic  $\pi$ -systems in the coplanar structure. However, considering the relatively low energy barrier between the two geometries, the XPS spectrum has been computed for both planar ( $\theta = 0^\circ$ ) and twisted ( $\theta = 42^\circ$ ) DEBP, in order to estimate the geometry dependence of the spectrum.

All calculations for the core-hole states have been performed at the ground state geometry by adopting contracted gaussian basis sets of triple zeta (TZ) quality consisting of 5s, 3p functions for C, N and O [28] and of double zeta quality for H [29]. For the two smallest molecules here considered, PA and PNPA, the effect of the basis set was investigated by performing calculations also with a larger basis set (PVTZ) obtained from the TZ basis set by adding a polarization d function on the heavy atoms and a third s function on H. As will be shown in details in the following section, the dependence of the computed BEs from the different basis sets can be simply described, for both

molecules, as a small common shift of all the BEs. The overall shape of the simulated spectra and the assignment of the observed spectral features did not change, so we avoided the computer time consuming calculations with the PVTZ basis set for the larger (DEBP, DPBD) molecules. It should be pointed out that in order to improve convergence to the correct core-hole state, the initial guess of the half-occupied orbital in the core-hole SCF calculation was obtained from the ground state orbitals by a localization procedure around the ionization site of interest.

The theoretical simulation of an XPS spectrum requires, of course, not only the knowledge of the energy position (BE) of each peak contributing to the spectrum, but also the knowledge of the corresponding intensity. The explicit calculation of such intensity is, in general, a difficult task requiring the evaluation of a dipole matrix element between the ground state and the final continuum state. However for X-ray excitation well above the ionization thresholds, as in the present measurements where photoelectrons of kinetic energy of about 50 eV were collected, the variation of such dipole matrix element for the different ionization sites is quite small. We can then assign the same nominal value (1) of intensity to each ionization process and present the theoretical spectrum as a bar diagram (see Fig. 2) where the intensity of each peak is simply proportional to the multiplicity of the ionization site.

In order to have an easier comparison with the experimental spectra, we also performed a convolution of such bar diagrams with a gaussian function of full width at half maximum FWHM = 0.5 eV that is intended to reproduce the broadening of the experimental peaks due mostly to molecular vibrations and limited instrumental resolution. The use of a gaussian function here, as well as in our attempt, discussed in the following section, of deconvoluting the experimental spectra, is evidently arbitrary. The effective vibrational line shape of an XPS peak could certainly be more complex and asymmetric and give origin to a substantially different distribution of intensity, compared to that described by a gaussian function. However, because the measured spectra show large unresolved peaks and detailed information on the

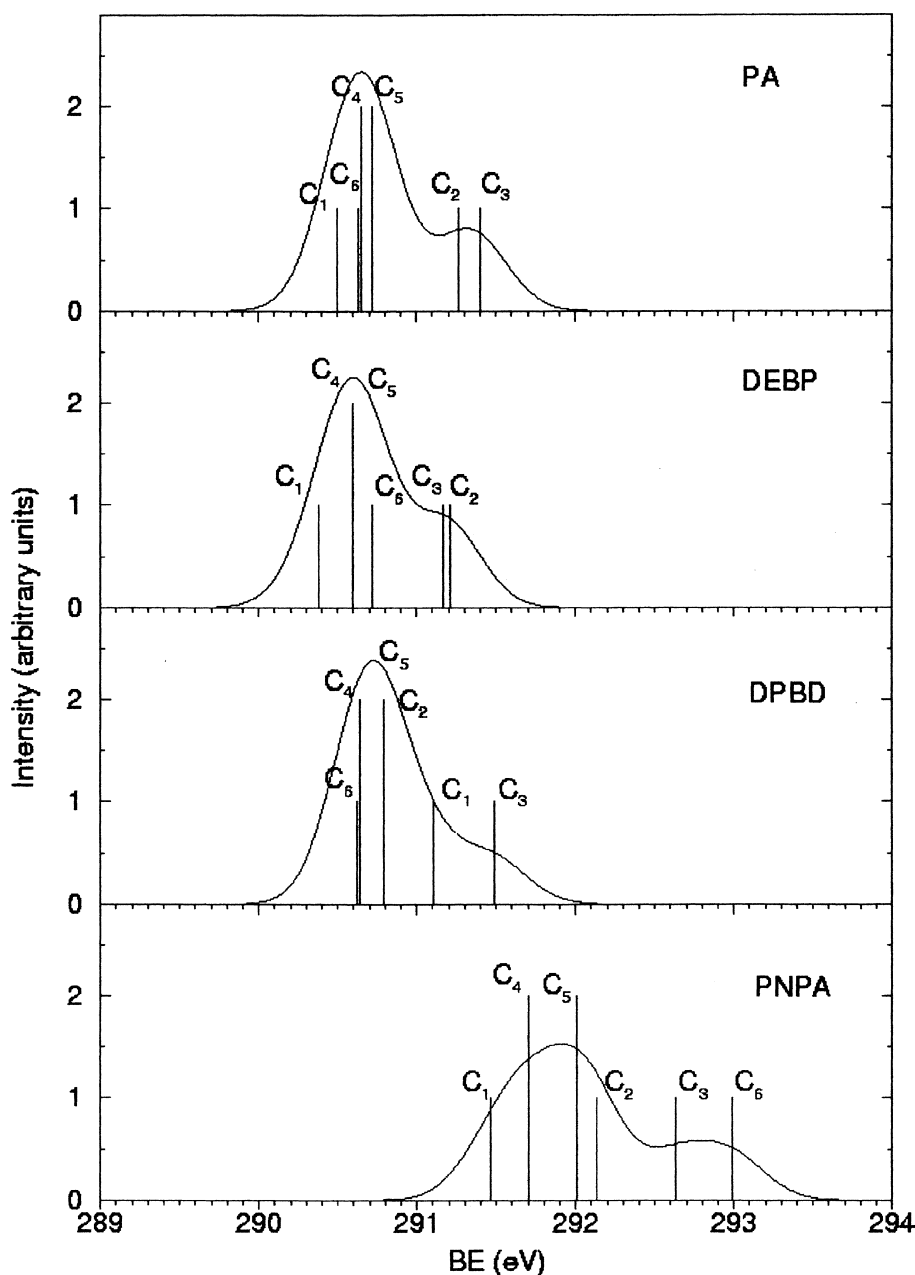


Fig. 2. Calculated BEs (bar diagrams), using the basis set TZ, and their convolution (continuous lines) with a gaussian function of FWHM = 0.5 eV for the investigated molecules; the labels of the peaks refer to the numbering of the carbon atoms in Fig. 1.

vibrational motion of these large molecules is not available, we believe that a gaussian function may be considered a reasonable approximation of the vibrational lineshape. The effective vibrational line

shape of an XPS peak could certainly be more complex and asymmetric (see for instance Ref. [30] and references therein) and give origin to larger or asymmetric peaks.

#### 4. Results and discussion

Table 1 shows the calculated C1s BEs for all the six non-equivalent sets of carbon atoms (see Fig. 1 for labels) of the investigated molecules PA, DEBP, DPBD and PNPA; for PA and PNPA two different basis sets were used (TZ and PVTZ), as described in Section 3, and the results of both calculations are shown in the table. The calculated

BEs for benzene and acetylene by using the PVTZ basis set are also shown in Table 1 for comparison. Fig. 2 shows the calculated spectra of the four investigated systems. The bar diagrams are obtained from the calculated BEs assuming a nominal intensity value of 1 for each ionization site, while the continuous lines represent their convolution with a gaussian function (FWHM = 0.5 eV).

Table 1  
Calculated BEs of the six non-equivalent carbon atoms of the four investigated molecules<sup>a</sup>

C	PVTZ	−0.3 eV	TZ	−0.5 eV	Fit
PA					
C1	290.12	289.82	290.50	290.00	289.75
C2	290.79	290.49	291.26	290.76	290.55
C3	291.37	291.07	291.40	290.90	290.88
C4	290.42	290.12	290.65	290.15	
C5	290.49	290.19	290.72	290.22	290.16
C6	290.49	290.19	290.63	290.13	
C	PVTZ	−0.7 eV	TZ	−1.0 eV	Fit
PNPA					
C1	291.17	290.47	291.45	290.45	290.39
C2	291.75	291.05	292.12	291.12	291.39
C3	292.30	291.60	292.63	291.63	291.67
C4	291.45	290.75	291.70	290.70	290.82
C5	291.72	291.02	292.01	291.01	291.06
C6	292.59	291.89	292.98	291.98	291.95
C	TZ $\theta = 0^\circ$	−0.5 eV	TZ $\theta = 42^\circ$	−0.5 eV	Fit
DEBP					
C1	290.33	289.83	290.38	289.88	289.90
C2	291.56	291.06	291.21	290.71	290.65
C3	291.17	290.67	291.17	290.67	
C4	290.60	290.10	290.60	290.10	
C5	290.60	290.10	290.60	290.10	290.10
C6	290.79	290.29	290.70	290.20	
C	TZ $\theta = 0^\circ$	−0.6 eV	Fit		
DPBD					
C1	291.11	290.51	290.55		
C2	290.79	290.19	290.19		
C3	291.49	290.89	290.86		
C4	290.64	290.04	290.00		
C5	290.79	290.19	290.19		
C6	290.62	290.02	290.00		

Reference molecules, PVTZ: Acetylene – 291.47; Benzene – 290.39.

<sup>a</sup> For PA and PNPA, the results of both PVTZ and TZ basis set calculations are shown; for DEBP and DEBP only TZ calculations have been performed but for the DEBP molecule two different geometries, planar ( $\theta = 0^\circ$ ) and twisted ( $\theta = 42^\circ$ ), were investigated. The PVTZ-calculated BEs of acetylene and benzene are also shown for comparison. The calculated BE values have also been shifted (see third and fifth column), as described in the text, for an easier comparison with the experimental data derived from the deconvolution (fit).

In a rough building block approach, the PA molecule can be considered as resulting from the link between the “benzene” and the “acetylene” subunits. The comparison between the calculated BEs for the six non-equivalent carbon atoms of PA (PVZT basis set) and the BEs of the two subunits benzene and acetylene reveals an electron donation from the benzene ring to the carbons of the triple bond C1 and C2. The negative chemical shift of the BEs of the alkyne carbons of PA compared to the acetylene molecule ( $-1.35$  and  $-0.68$  for C1 and C2 respectively) results from a more effective electronic relaxation around the core hole created in the photoemission process, withdrawing electron charge from the benzene ring. The effect is stronger for C1 than for C2, as already discussed in Ref. [21]. A parallel antiscreening effect is found for the benzene carbons of PA, and in particular for C3, whose BE is  $0.98$  eV higher than the calculated BE for benzene, while the BEs of the other five benzene carbons C4–C6 appear almost unperturbed by the interaction with the triple bond. The results of calculations using

the smaller TZ basis set are also shown in Table 1. For both basis sets a shift is observed between the experimental spectrum and the calculated spectra ( $+0.3$  eV for PVTZ and  $+0.5$  eV for TZ basis set). This is due, mainly, to the neglected correlation energy, but, evidently, also from a limited basis set dependence in the description of the electron relaxation. However, the corrected BEs, also shown in Table 1, appear quite similar for the two basis sets employed and the basis set dependence does not prevent a univocal assignment of the observed spectral features.

The experimental C1s core-level spectrum of gas phase PA, reported in Fig. 3, apparently consists of four different contributions: a main photoemission peak at  $290.2$  eV, a strong shoulder at about  $290.9$  eV, a second shoulder barely visible on the high BE side of the main photoemission peak and a third shoulder on the low BE side. In order to check the correspondence between the calculated and measured spectra, we have attempted a curve-fitting deconvolution of the experimental spectra. The gaussian functions used as

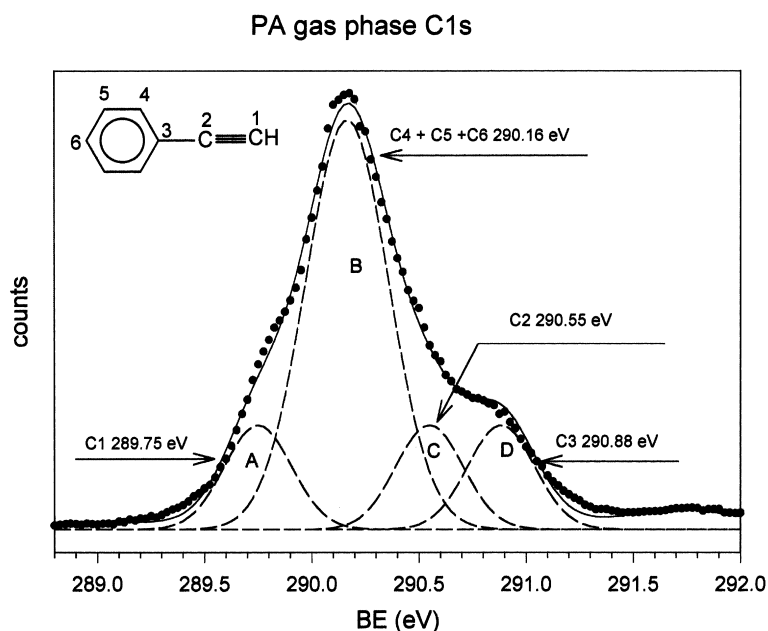


Fig. 3. Curve-fitting analysis of the C1s spectrum of gas phase PA; markers represent experimental points, dashed lines fitting components (labeled A–D in the figure), the continuous line the calculated spectrum; the BEs of the fitting component peaks are also indicated in the figure.



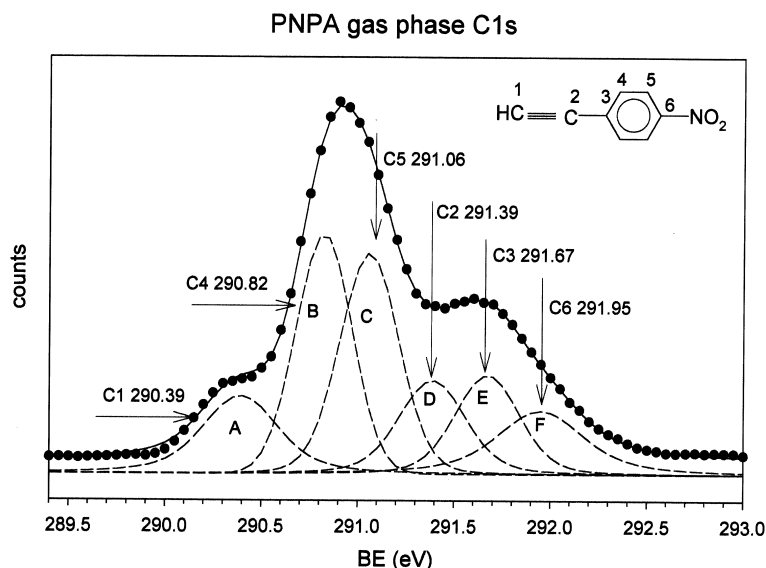


Fig. 4. Curve-fitting analysis of the C1s spectrum of gas phase PNPA; markers represent experimental points, dashed lines fitting components (labeled A–F in the figure), the continuous line the calculated spectrum; the BEs of the fitting component peaks are also indicated in the figure.

fitting components have approximately the same BE of the calculated peaks, after a proper “rigid” shift of the overall calculated spectrum by a fixed amount, as indicated in Table 1. The four peaks labeled A–D in Fig. 3 correspond, respectively, to: the highly screened alkyne carbon C1 (peak A), the benzene-like carbons C4–C6 (peak B), the alkyne carbon C2 (peak C) and the highly antiscreened benzene carbon directly bonded to the alkyne group C3 (peak D). The peak areas have been kept fixed, so that their ratio is A:B:C:D = 1:5:1:1, as expected on the basis of the chemical structure of PA. Moreover, the full width at half maximum (FWHM) has been assumed to be the same (0.35 eV) for peaks A, C and D, while peak B, resulting from the superimposition of the signals of carbons 4–6, is assumed to be a little bit larger (0.45 eV). A good overall agreement is found between the calculated BEs and the energy position (shown in Fig. 3 and in Table 1) of the four gaussian peaks obtained by the best fit of the experimental spectrum. Actually, the calculations based on the PVTZ basis set seem to overestimate the BE of C3, while the TZ basis set overestimates the BEs of C1 and C2; in both cases, however, the mismatch between experiment and theory is rather small (0.2 eV).

Fig. 4 shows the C1s spectrum of gas phase *para*-nitrophenylacetylene or PNPA; the measured spectrum resembles the C1s spectrum of PA but it is shifted of about +0.5 eV with respect to the PA spectrum and presents a stronger and larger shoulder on the high BE side; both phenomena are evidently connected with the presence of the highly electron withdrawing nitro-group. The BE values calculated by means of TZ and PVTZ basis sets are displayed in Table 1 and clearly evidence the electron withdrawing effect of the nitro-group. The influence of the nitro group is stronger, as expected, for the carbon atom C6 directly bonded to the substituent, but it is also relevant for the other BEs, leading to chemical shifts that cover a larger energy range. In particular, we observe a strong variation of the BEs of the two carbons C5 in the *ortho* position, so that the BE degeneration of the benzene carbons C4–C6 present in the PA molecule is completely removed. The comparison of calculated and measured spectra gives an average shift of +0.7 eV for PVTZ basis set and of +1.0 eV for TZ basis set; in both cases, higher than the one observed for PA. We have attempted a curve-fitting analysis of the experimental spectrum on the basis of the calculated BEs, by using six fitting

components, labeled A–F in Fig. 4 and corresponding, respectively, to the carbon atoms C1 (A), C4 (B), C5 (C), C2 (D), C3 (E) and C6 (F). Again, we have kept the area ratio between the fitting components fixed, and corresponding to A:B:C:D:E:F = 1:2:2:1:1:1, as expected on the basis of the molecular structure. A good agreement is found between the BEs of the fitting components (shown in Table 1) and the BEs calculated using both basis set, after proper correction, with the only exception of C2, whose BE appears to be slightly underestimated (−0.2 eV) by the calculation using both basis sets. In order to obtain a good fit of the experimental data, peak F, corresponding to carbon C6, must be supposed to be larger (FWHM = 0.5 eV) than the other peaks (FWHM = 0.35 eV), possibly due to different vibrational broadening effects.

For the larger molecules DEBP and DBPD, that can be considered as dimers of the PA molecule, calculations have been performed only with the TZ basis set and the results are shown in Table 1. Concerning the DEBP molecule, consisting of

two PA units linked together through the benzene carbons C6, theoretical calculations have been performed for two different geometries, depending on the torsion angle ( $\theta = 42^\circ$  and  $\theta = 0^\circ$ ) between the benzene rings of the two PA subunits.

The experimental spectrum of gas-phase DEBP is shown in Fig. 5. It is evidently less structured than the one of PA in Fig. 3 and appears essentially as a single large symmetric band centered around 290.2 eV. The calculations performed for the twisted ( $\theta = 42^\circ$ ) DEBP geometry (see Fig. 2) resulted to be more appropriate for this molecule, producing a spectrum more similar to the expected one than the “planar” DEBP configuration ( $\theta = 0^\circ$ ). The obtained results show that the difference between PA and DEBP spectra are mainly due to different chemical shifts of the C atoms (C3, C6) involved in the subunits bonding. We have also attempted to perform a curve-fitting deconvolution of the spectrum on the basis of the calculated BEs for twisted DEBP. The first gaussian on the low energy side, labeled A in Fig. 5, corresponds to the highly screened alkyne carbon C1,

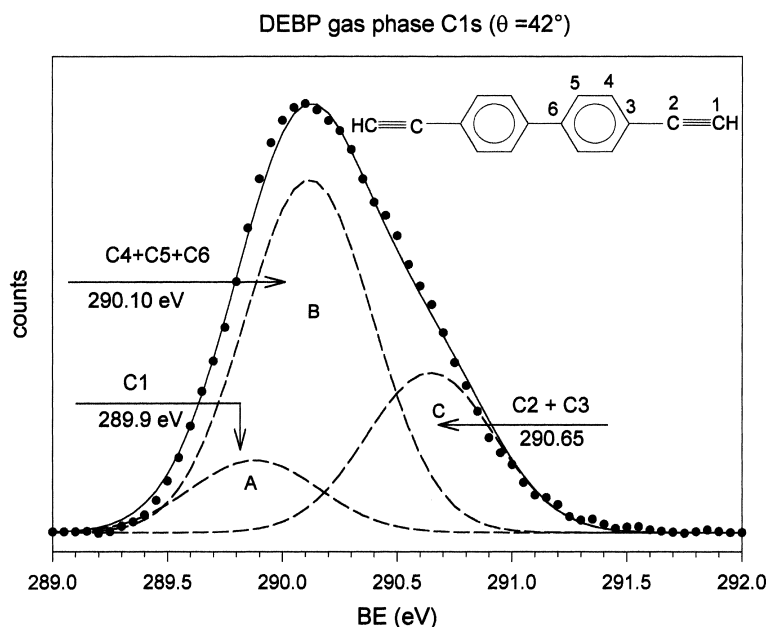


Fig. 5. Curve-fitting analysis of the C1s spectrum of gas phase DEBP; markers represent experimental points, dashed lines fitting components (labeled A–C in the figure), the continuous line the calculated spectrum; the BEs of the fitting component peaks are also indicated in the figure.

the central peak (B) to the benzene carbons C4–C6, while the third high BE component (C) is considered to collect the intensity of the alkyne carbon C2 and of the highly antiscreened benzene carbon C3, directly bonded to the alkyne group. The energy position of the best fitting peaks, shown in Fig. 5 and Table 1 are in good agreement with the calculated C1s ionization potentials (again, with an energy shift of +0.5 eV between experiment and theory). Also in this case the fit has been performed assuming that the area ratio should be A:B:C = 1:5:2, as expected on the basis of the molecular structure.

The DPBD molecule, on the other hand, consists of two PA-like subunits linked together through the C1 carbons of the triple bond. The optimised geometry for DPBD predicts a torsion angle between the two subunits of about 10°, i.e. almost planar. On the basis of the observed negligible dependence of the computed spectrum of DEBP from the torsion angle, and with the purpose of taking advantage of the higher symmetry, the BEs have been calculated for a planar ( $\theta = 0^\circ$ )

DPBD molecule and the results are collected in Table 1. Comparing the BEs calculated for DPBD to those of PA (TZ basis set), we deduce a perturbation of the electron density distribution around the carbons C1 and C2, with a marked increase in the BE of C1 (+0.61 eV) and a parallel decrease (−0.47 eV) for C2. For C1, the  $\sigma$ -bonding with the alkyne group seems to have an anti-screening effect, as already evidenced for C3 in the PA molecule. The screening effect observed for C2 can be related to the possibility of a charge-density withdrawal from the benzene ring of the other PA subunits, upon formation of a core hole in a C2 atom; this effect can be explained in terms of resonance structures.

The experimental spectrum of DPBD and its curve-fitting deconvolution are shown in Fig. 6. Four fitting components have been employed, labeled A–D in the figure and corresponding respectively to carbons C4 + C6 (A), C5 + C3 (B), C1 (C) and C2 (D); their BEs are shown in Table 1. In order to obtain a good correspondence between the BEs of the fitting components and the calcu-

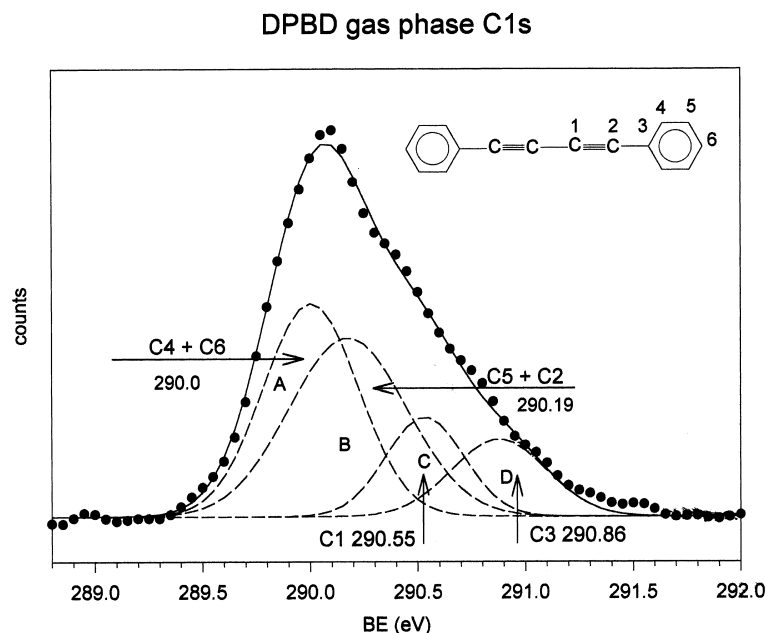


Fig. 6. Curve-fitting analysis of the C1s spectrum of gas phase DPBD; markers represent experimental points, dashed lines fitting components (labeled A–D in the figure), the continuous line the calculated spectrum; the BEs of the fitting component peaks are also indicated in the figure.

lated values for the corresponding carbon atoms, the last ones had to be shifted by approximately  $-0.6$  eV. The area ratio between the fitting components has been kept fixed and is A:B:C:D = 3:3:1:1, as expected on the basis of the chemical structure of DPBD.

## 5. Conclusions

The C1s core level photoemission spectra of a series of aromatic compounds have been interpreted with the help of quantum chemical *ab initio* calculations. The assignment of the various features present in the spectrum allowed to shed light on the influence of the  $\sigma$ -bonding between the benzene and the alkyne groups on the relaxation processes taking place around the C1s core hole in all the six non-equivalent atoms of the investigated molecules.

In the PA molecule, the core holes around the alkyne carbons C1 and C2 are stabilized by the electron donation from the benzene ring; in parallel, the interaction with the alkyne group produces an antiscreening effect on the core hole of the benzene carbon C3. When a nitro group is introduced in the benzene ring in the *para* position (PNPA), the electron withdrawing effect of the substituent generates an increase in the BEs of all the six non-equivalent carbon atoms; this effect is more pronounced for the benzene carbon C6 directly bonded to the substituent and for the carbons C5 in the *ortho* position.

In the larger DEBP and DPDB molecules, the link between the two PA subunits produces a rearrangement of the overall charge distribution. In the DEBP molecule an angle of  $42^\circ$  is found between the two PA subunits linked together through the aromatic rings in the *para* position; as a result of a reduced conjugation between the two  $\pi$ -systems, relatively small changes of the BEs are detected. Larger effects are evidenced in the DPBD molecule, consisting of two PA subunits linked together through the triple bonds with an angle of  $10^\circ$ , i.e. almost coplanar. A strong rearrangement of the electron density around the core hole of the triple bond carbons C1 and C2, with respect to PA, is evidenced, with a remarkable increase in the

BE of the carbon C1, linked to the triple bond of the other subunit, and a parallel decrease of the BE of carbon C2.

We plan to extend our investigations to the NEXAFS spectra of the reported organic molecules (NEXAFS spectra of PA have already been reported [21], investigations on DEBP are in progress). In this framework, we think that the information obtained by XPS spectroscopy and by comparison with theoretical calculations on the ionization potentials of the non-equivalent carbons of the investigated systems will be extremely helpful in the interpretation of the NEXAFS spectra. Our final goal is to use the information obtained in the XPS and NEXAFS spectroscopy study on the model molecules in the interpretation of the NEXAFS spectra of the polymeric systems [9,17].

## Acknowledgements

We would like to thank CNR PF-MSTA II and MURST for financial support, Dr. Rosaria D'Amato for supplying *para*-nitrophenylacetylene, Elettra staff and colleagues at the Gas Phase Beamline for support during the experiment.

## References

- [1] P. Ehrlich, W.A. Anderson, in: T.A. Skotheim (Ed.), *Handbook of Conducting Polymers*, vol. 2, Marcel Dekker, New York, 1986, p. 441.
- [2] A. Furlani, M.V. Russo in: J.C. Salamone (Ed.), *Polymeric Materials*, vol. 8, CRC Press, New York, 1996, p. 6841.
- [3] A. Bearzotti, V. Foglietti, G. Polzonetti, G. Iucci, A. Furlani, M.V. Russo, *Mater. Sci. Engng. B* 40 (1996) 1.
- [4] C. Caliendo, E. Verona, A. Furlani, G. Iucci, M.V. Russo, *Sens. Actuat. B* 18–19 (1994) 82.
- [5] D. Neher, A. Wolf, C. Bubeck, G. Wegner, *Chem. Phys. Lett.* 163 (1989) 116.
- [6] M.V. Russo, G. Iucci, A. Furlani, A. Camus, N. Marsich, *Appl. Organomet. Chem.* 5 (1992) 517.
- [7] M.V. Russo, A. Furlani, R. D'Amato, *J. Polym. Sci.: Part A: Polym. Chem.* 36 (1998) 93.
- [8] G. Polzonetti, M.V. Russo, A. Furlani, G. Iucci, *Chem. Phys. Lett.* 185 (1991) 105.
- [9] G. Polzonetti, V. Carravetta, M.V. Russo, G. Contini, P. Parent, C. Laffon, *J. Electron. Spectrosc. Relat. Phenom.* 98–99 (1999) 175.

- [10] G. Polzonetti, M.V. Russo, G. Iucci, A. Furlani, *Synth. Met.* 55–57 (1993) 165.
- [11] G. Polzonetti, M.V. Russo, G. Iucci, A. Furlani, *Appl. Surf. Sci.* 72 (1993) 227.
- [12] G. Polzonetti, M.V. Russo, A. Furlani, G. Infante, *Chem. Phys. Lett.* 214 (1993) 333.
- [13] C. Frazier, S. Guha, W.P. Chen, M.P. Cockerman, P.L. Porter, E.A. Chanchard, C.H. Lee, *Polymer* 28 (1987) 553.
- [14] N. Chawdhury, A. Köhler, R.H. Friend, M. Youms, N.Y. Long, P.R. Raithby, J. Lewis, *Macromolecules* 31 (1998) 722.
- [15] C. Caliendo, E. Verona, A. D'Amico, A. Furlani, G. Infante, M.V. Russo, *Sensors Actuat. B* 24–25 (1995) 67.
- [16] G. Polzonetti, G. Iucci, C. Furlani, M.V. Russo, A. Furlani, G. Infante, G. Paolucci, B. Brena, D. Cocco, *Chem. Phys. Lett.* 267 (1997) 384.
- [17] M.V. Russo, G. Infante, G. Polzonetti, G. Contini, G. Tourillon, Ph. Parent, C. Laffon, *J. Electron. Spectrosc. Relat. Phenom.* 85 (1997) 53.
- [18] G. Beamson, D. Briggs, *Mol. Phys.* 76 (1992) 919.
- [19] A. Naves de Brito, N. Correia, S. Svensson, H. Ågren, *J. Chem. Phys.* 95 (1991) 2965.
- [20] A. Naves de Brito, S. Svensson, H. Ågren, J. Delhalle, *J. Electron. Spectrosc. Relat. Phenom.* 63 (1993) 239.
- [21] V. Carravetta, G. Polzonetti, G. Iucci, M.V. Russo, G. Paolucci, *Chem. Phys. Lett.* 288 (1998) 37.
- [22] M.V. Russo, A. Furlani, G. Infante, E. Muraglia, G. Sleiter, *Proc. Adv. Synth. Methodol. Inorg. Chem.* 1 (1991) 258.
- [23] S. Takahashi, Y. Kuroyama, K. Sonogashira, N. Hagihara, *Synthesis* (1980) 327.
- [24] A. Unchida, T. Nakazawa, I. Kondo, N. Iwata, S. Matsuda, *J. Org. Chem.* 37 (1972) 3749.
- [25] S. Takahashi, Y. Kuroyama, K. Sonogashira, N. Hagihara, *Synthesis* (1980) 627.
- [26] R.R. Blyth, R. Delaunay, M. Zitnik, J. Krempasky, R. Krempaska, J. Slezak, K.C. Prince, R. Richter, M. Vondracek, R. Camilloni, L. Avaldi, M. Coreno, G. Stefani, C. Furlani, M. de Simone, S. Stranges, M.Y. Adam, *J. Electron. Spectrosc. Relat. Phenom.* 101–103 (1999) 959.
- [27] T. Helgaker, H.J.A. Jensen, P. Joergensen, J. Olsen, K. Ruud, H. Ågren, T. Andersen, K.L. Bak, V. Bakken, O. Christiansen, P. Dahle, E.K. Dalskov, T. Enevoldsen, H. Heiberg, H. Hettema, D. Jonsson, S. Kirpekar, R. Kobayashi, H. Koch, K.V. Mikkelsen, P. Norman, M.J. Packer, T. Saue, P.R. Taylor, O. Vahtras, DALTON, an ab initio electronic structure program, Release 1.0, 1997.
- [28] T.H. Dunning Jr., *J. Chem. Phys.* 55 (1971) 716.
- [29] T.H. Dunning Jr., P.J. Hay, in: H.F. Shaefer III (Ed.), *Methods of Electronic Structure Theory*, Plenum Press, New York, 1977, p. 1.
- [30] O. Plashkevych, T. Privalov, H. Ågren, V. Carravetta, K. Ruud, *Chem. Phys.* 260 (2000) 11.